Annals of Physics 363 (2015) 305–315

Contents lists available at ScienceDirect

Annals of Physics

journal homepage: www.elsevier.com/locate/aop

Automatic Fourier transform and self-Fourier beams due to parabolic potential

Yiqi Zhang [a,*], Xing Liu [a], Milivoj R. Belić [b,*], Weiping Zhong [c], Milan S. Petrović [d], Yanpeng Zhang [a,*]

[a] Key Laboratory for Physical Electronics and Devices of the Ministry of Education & Shaanxi Key Lab of Information Photonic Technique, Xi'an Jiaotong University, Xi'an 710049, China

[b] Science Program, Texas A&M University at Qatar, P.O. Box 23874 Doha, Qatar

[c] Department of Electronic and Information Engineering, Shunde Polytechnic, Shunde 528300, China

[d] Institute of Physics, P.O. Box 68, 11001 Belgrade, Serbia

ARTICLE INFO

Article history:
Received 1 June 2015
Accepted 6 October 2015
Available online 22 October 2015

Keywords:
Parabolic potential
Self-Fourier beam

ABSTRACT

We investigate the propagation of light beams including Hermite–Gauss, Bessel–Gauss and finite energy Airy beams in a linear medium with parabolic potential. Expectedly, the beams undergo oscillation during propagation, but quite unexpectedly they also perform automatic Fourier transform, that is, periodic change from the beam to its Fourier transform and back. In addition to oscillation, the finite-energy Airy beams exhibit periodic inversion during propagation. The oscillating period of parity-asymmetric beams is twice that of the parity-symmetric beams. Based on the propagation in parabolic potential, we introduce a class of optically-interesting beams that are self-Fourier beams—that is, the beams whose Fourier transforms are the beams themselves.

1. Introduction

It is well known that a light beam undergoes discrete diffraction while propagating in a waveguide array, and that such a diffraction is prohibited when the refractive index of the waveguide array

* Corresponding authors.
E-mail addresses: zhangyiqi@mail.xjtu.edu.cn (Y.Q. Zhang), milivoj.belic@qatar.tamu.edu (Milivoj R. Belić), ypzhang@mail.xjtu.edu.cn (Y.P. Zhang).

http://dx.doi.org/10.1016/j.aop.2015.10.006
0003-4916/

is appropriately modulated [1,2]. The phenomenon is linear, that is, obtained without invoking nonlinearity in the paraxial wave equation [3]. Likewise, in free space or a linear bulk medium a light beam will diffract unless it belongs to the family of nondiffracting beams [4,5]—a class of linear beams that attracted a lot of attention in the past few years. A celebrated member of this class is the Airy beam [4,6–10]. In optics, ways to effectively modulate light beams have always been high on research agenda. As an effective tool, a photonic potential – a "potential" embedded in the medium's index of refraction—is often used in linear optics and extensively referenced in the literature. It comes in different forms, as exemplified by vastly different photonic crystal structures. A linear potential which affects the properties of an Airy plasmon beam and is used to control acceleration of Airy beams has been reported in [11,12]. An external longitudinally-dependent transverse potential will modulate the propagating trajectory of the light beam according to the form of the potential [13]. In Refs. [14–16] authors discussed the propagation and transformation of finite-energy Airy beams in a linear medium with a parabolic potential, in which periodic inversion, oscillation, and phase transition were reported. One should recall that in a parabolic potential, light propagation is equivalent to a fractional Fourier transform (FT) [17], the fact first noted by Mendlovic and his collaborators [18,19]. The fractional FT can be conveniently introduced through the propagation in gradient-index (GRIN) media, which can further be connected with the propagation in the parabolic potential and the automatic FT—as done in this article. By now, beam propagation in GRIN media has matured to a proper part of optics that is best surveyed from a dedicated monograph [20]. In a nonlinear medium, the strongly nonlocal nonlinearity can be cast into a parabolic-like potential [21] and consequently the corresponding modulation effects more easily investigated [22–24].

In this article, we investigate the light beam management by a parabolic potential in a linear medium, theoretically and numerically. The program presented extends the traditional Fourier optics, which deals with the free-space propagation, to the realm of propagation in a parabolic potential. Since such a potential causes harmonic oscillation of light beams, it is interesting to investigate the influence of the potential on the dynamics of useful light beams, such as Hermite–Gauss (HG), Bessel–Gauss (BG), and finite energy Airy beams (ABs). Even though there are many papers dealing with the parabolic potential and linear harmonic oscillation, we believe that results obtained here have not been reported before, to the best of our knowledge.

The organization of the article is as follows. In Section 2, we describe the problem and introduce the theoretical model of beam propagation. In Section 3, we discuss the repercussions of the model on the dynamics of the beams mentioned. In Section 4, we solve the model, obtain analytical solutions, and analyze those solutions. Based on the theoretical model, we discover a class of interesting self-Fourier beams and present them in Section 5. Section 6 concludes the paper.

2. Theoretical model

The paraxial propagation of a beam in a linear medium with an external parabolic potential, is described by the dimensionless Schrödinger equation

$$i\frac{\partial\psi}{\partial z}+\frac{1}{2}\frac{\partial^2\psi}{\partial x^2}-\frac{1}{2}\alpha^2x^2\psi=0, \tag{1}$$

where x and z are the normalized transverse coordinate and the propagation distance, respectively, scaled by some transverse width x_0 and the corresponding Rayleigh range kx_0^2. Here, $k=2\pi n/\lambda_0$ is the wavenumber, n the index of refraction, and λ_0 the wavelength in vacuum. Parameter α scales the width of the potential. For our purposes, the values of parameters can be taken as $x_0=100\,\mu$m, $n=1.45$, and $\lambda_0=600$ nm [25,26].

Eq. (1) has many well-known solutions; we utilize the ones that are of interest in the paraxial beam propagation. But before selecting any solutions, we perform the Fourier transform (FT) of Eq. (1), to obtain

$$i\frac{\partial\hat{\psi}}{\partial z}+\frac{1}{2}\alpha^2\frac{\partial^2\hat{\psi}}{\partial k^2}-\frac{1}{2}k^2\hat{\psi}=0, \tag{2}$$

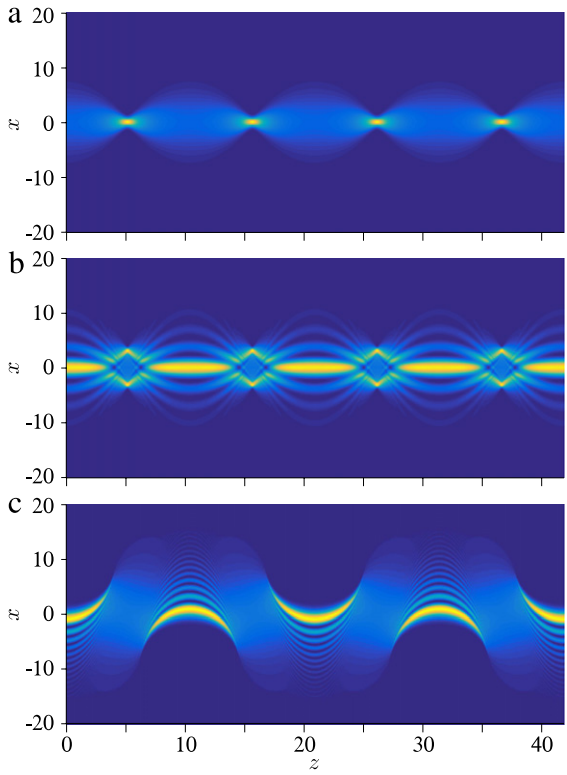

Fig. 1. (Color online) Propagation of beams in a linear medium with parabolic potential. (a) Hermite–Gauss beam, with input $\psi(x) = \exp(-x^2/2\sigma^2)H_0(x/\sigma)$ with $\sigma = 5$. (b) Bessel–Gauss beam, input $\psi(x) = \exp(-x^2/2\sigma^2)J_0(x)$ with $\sigma = 10$. (c) Finite energy Airy beam, input $\psi(x) = \exp(ax)\mathrm{Ai}(x)$. The parameters are $a = 0.1$ and $\alpha = 0.3$.

where the FT is defined as

$$\hat{\psi} = \int_{-\infty}^{+\infty} \psi e^{-ikx} dx, \qquad \psi = \frac{1}{2\pi} \int_{-\infty}^{+\infty} \hat{\psi} e^{ikx} dk.$$

Obviously, Eq. (2) can be put in the same form as Eq. (1), especially if $\alpha = 1$. Both equations can have the same solutions but expressed in different spaces, real and inverse. The eventual differences in solutions come to the fore once the equations are presented as boundary-value problems in specific physical settings. Also, Eqs. (1) and (2) indicate that localized light beams in real (x) and inverse (k) spaces may share the same dynamics from a mathematical point of view. Therefore, it is natural to consider the following scenario in linear optical setting for a beam propagating according to Eq. (1): (i) the beam undergoes FT during propagation, and then experiences an inverse FT, to reconstruct the initial beam; (ii) the process represented in (i) occurs periodically during propagation, and profile oscillation and recurrence take place along the propagation direction.

The scenario outlined resembles a repeating $4f$ correlator system from Fourier optics, except that it deals with the propagation in a parabolic potential. To present a realization of the scenario outlined, we display the propagation of HG, BG and a finite energy AB in Fig. 1(a)–(c), respectively. Clearly, the parabolic potential imposes simple harmonic oscillation on an HG beam, as shown in Fig. 1(a), prevents discrete-like diffraction of a BG beam (Fig. 1(b)), and causes periodic inversion of an AB (Fig. 1(c)). This inversion [14,15] is different from the inversion of an AB reported in fibers, when the third-order dispersion is taken into account [27], and from the double focusing of an AB in Ref. [28].

In Fig. 1(a) and (b), the initial beams are parity-symmetric, so an odd-integer multiple of half periods $\mathcal{D}_s$ of harmonic oscillation is needed for the beam to realize its FT. However, in Fig. 1(c) the

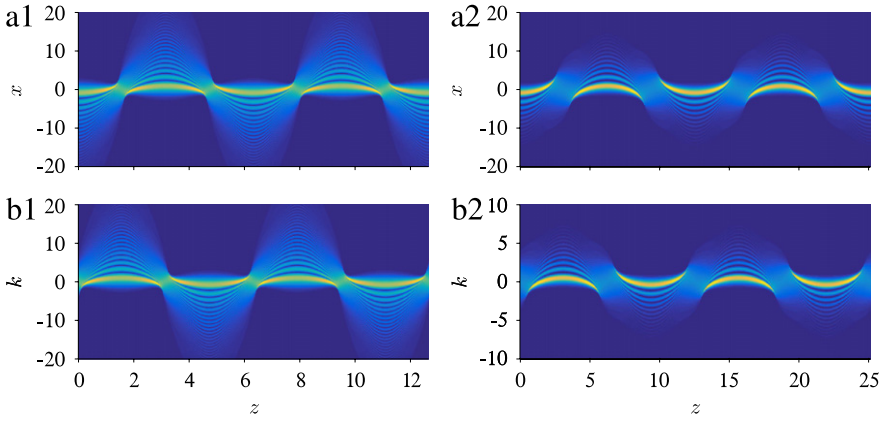

Fig. 2. (Color online) Periodic inversion and automatic Fourier transform of a finite energy Airy beam during propagation. (a) Real space. (b) Inverse space. The parameters are: $a = 0.1$, $\alpha = 1$ and $\alpha = 0.5$ for the left panels and the right panels, respectively.

initial beam is parity-asymmetric, so it inverts once before reconstruction; as a result, the relation between oscillation periods of symmetric and asymmetric beams is $\mathcal{D}_{\rm as} = 2\mathcal{D}_s$. The corresponding FTs are located at an integer multiple of $(2m-1)\mathcal{D}_{\rm as}/4$, with m being an even integer. If m is an odd integer, the rule gives the FT of the finite energy AB at inversion. This demonstrates that HG, BG, and finite energy ABs perform an automatic Fourier transformation, which means that the FT of these beams will appear automatically and periodically during propagation, based on this simple model.

3. Discussion

In this section, we address the properties of the three beams during propagation. Specifically, in Fig. 2 we depict the periodic inversion and automatic FT of an AB during propagation. In Fig. 2(a1) and (b1), $\alpha = 1$, so that the beam intensities in the real domain and the inverse domain are identical, but phase-shifted. In Fig. 2(a2) and (b2), $\alpha = 0.5$; therefore, there is a transverse scaling between the intensities in real and inverse domains. Using Parseval's theorem

$$\int_{-\infty}^{+\infty} |\psi(x)|^2 dx = \frac{1}{2\pi}\int_{-\infty}^{+\infty} |\hat{\psi}(k)|^2 dk$$

and a gauge transformation, we can obtain the FT of the three initial beams in real space.

For an arbitrary order HG beam $\psi(x,\ 0) = \exp(-x^2/2\sigma^2)H_n(x/\sigma)$, with n the order of Hermite polynomials (in Fig. 1(a), the order is 0),

$$\psi\left(x,\ z = \frac{m}{2}\mathcal{D}_s\right) = (-i)^n\sqrt{\alpha}\sigma\,\exp\left(-\frac{1}{2}\alpha^2\sigma^2x^2\right)H_n\left(\alpha\sigma x\right), \tag{3a}$$

where m is an odd integer. If we let $\alpha = 1$ and $\sigma = 1$, we find Eq. (3a) to coincide completely with the initial beam. The reason is that $\psi(x,\ 0) = \exp(-x^2/2)H_n(x)$ is an eigenmode of Eq. (1), which is a well known fact.

Concerning the BG beam, we also consider the general case $\psi(x,\ 0) = \exp(-x^2/2\sigma^2)J_n(x)$, with n being the order of the Bessel function. The corresponding FT can be obtained as a convolution of FTs of the Gauss and Bessel functions. After some algebra, one obtains

$$\psi\left(x,\ z = \frac{m}{2}\mathcal{D}_s\right) = (-i)^n\frac{\sigma\sqrt{\alpha}}{\pi}\int_{-\pi/2}^{\pi/2} T_n(\sin\theta)\exp\left[-\frac{\sigma^2}{2}\left(\alpha x - \sin\theta\right)^2\right]d\theta, \tag{3b}$$

where T_n is the Chebyshev polynomial of the first kind. For the case in Fig. 1(b), $n = 0$.

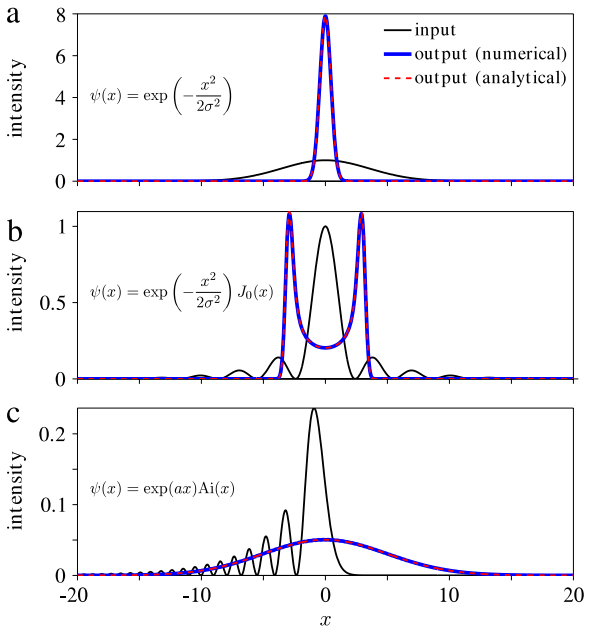

Fig. 3. (Color online) Comparison between numerical and analytical results. (a)–(c) Corresponding to Fig. 1(a)–(c), respectively; outputs are taken at $z = \mathcal{D}_s/2$, $\mathcal{D}_s/2$, and $3\mathcal{D}_{as}/4$. Perfect agreement is visible.

The case of an AB is more interesting, but also more involved. Since the FT of $\psi(x) = \mathrm{Ai}(x)\exp(ax)$ is

$$\hat{\psi}(k) = \exp(-ak^2)\exp\left[\frac{a^3}{3} + \frac{i}{3}\left(k^3 - 3a^2k\right)\right],$$

the beam envelope can be written as

$$\psi\left(x,\, z = \frac{2m-1}{4}\mathcal{D}_{as}\right) = \sqrt{-\frac{s\alpha}{2\pi}}\exp\left(-\alpha^2 a x^2 + i\frac{\pi}{4}\right) \times \exp\left[\frac{a^3}{3} + i\frac{s}{3}\left(\alpha^3x^3 - 3\alpha a^2 x\right)\right]. \tag{3c}$$

In Eq. (3c), $s = 1$ if m is odd and $s = -1$ if m is even. It will be verified later in the article that the oscillation period is

$$\mathcal{D}_s = \frac{\pi}{\alpha} \tag{4a}$$

for parity symmetric beams (e.g., HG and BG), and

$$\mathcal{D}_{as} = \frac{2\pi}{\alpha} \tag{4b}$$

for beams lacking parity symmetry (e.g., ABs).

Analytical solutions given by Eqs. (3a)–(3c) completely agree with the numerical simulations displayed in Figs. 1 and 2, as shown in Fig. 3. From Eqs. (3a)–(3c), (4a) and (4b), one can see that the harmonic oscillation, self-Fourier transform and periodic inversion are only dependent on α; apodization factors σ and a do not affect these phenomena.

Thus far, we have found analytical expressions of propagating beams at certain distances; the procedure may also be applied to other kinds of initial light beams, regardless of their parity symmetry. The question is, what happens in-between these specific distances.

4. Analytical solutions

We now go back to Eq. (1); as mentioned, it possesses many solutions. We select ones that are relevant for the study at hand, some of which are derived by the self-similar method [29–31]. Generally, the solution of Eq. (1) can be written using a kernel [32,33,14,15]

$$\psi(x,z)=\int_{-\infty}^{+\infty}\psi(\xi,0)\sqrt{\mathcal{H}(x,\xi,z)}d\xi, \tag{5}$$

where

$$\mathcal{H}(x,\xi,z)=-\frac{i}{2\pi}\alpha\csc(\alpha z)\exp\left\{i\alpha\cot(\alpha z)\left[x^2+\xi^2-2x\xi\sec(\alpha z)\right]\right\}. \tag{6}$$

Combining Eqs. (5) and (6), after some algebra one ends up with

$$\psi(x,z)=f(x,z)\int_{-\infty}^{+\infty}\left[\psi(\xi,0)\exp\left(ib\xi^2\right)\right]\exp(-iK\xi)d\xi, \tag{7}$$

where

$$b=\frac{\alpha}{2}\cot(\alpha z),\qquad K=\alpha x\csc(\alpha z),$$

and

$$f(x,z)=\sqrt{-\frac{i}{2\pi}\frac{K}{x}}\exp\left(ibx^2\right).$$

One can see that the integral in Eq. (7) is a FT of $\psi(x,0)\exp\left(ibx^2\right)$. Therefore, after choosing an input $\psi(x,0)$, one can get an analytical evolution solution by finding the FT of $\psi(x,0)\exp\left(ibx^2\right)$. In other words, the propagation of a beam in a parabolic potential is equivalent to a kind of automatic FT, that is, to the periodic change from the beam to the FT of the beam with a parabolic chirp and back. It is worth mentioning that Eq. (7) is a fractional FT of the initial beam [34,18,19], the "degree" of which is proportional to the propagation distance.

4.1. Hermite–Gauss beams

Corresponding to the case with $\psi(x,0)=\exp(-x^2/2\sigma^2)H_n(x/\sigma)$, that is, the HG beam, the solution can be written as

$$\psi(x,z)=f(x,z)\int_{-\infty}^{+\infty}\exp\left(-\beta\xi^2\right)H_n\left(\frac{\xi}{\sigma}\right)\exp(-iK\xi)d\xi, \tag{8}$$

where $\beta=1/(2\sigma^2)-ib$. Different from the fundamental HG beam, the general solution of Eq. (8) is nontrivial. However, (i) when $z=m\mathcal{D}_s/2$ with m an odd integer, the solution in Eq. (8) is reduced to Eq. (3a), the FT of the initial beam; (ii) given certain integer n, one can calculate the corresponding analytical solution. Specifically, if $n=0$, we have

$$\begin{aligned}\psi(x,z)&=f(x,z)\sqrt{\frac{\pi}{\beta}}\exp\left(-\frac{K^2}{4\beta}\right)\\&=f(x,z)\frac{\sqrt{2\pi}\sigma}{\sqrt{1-i\sigma^2\alpha\cot(\alpha z)}}\exp\left(-\frac{\alpha^2\sigma^2x^2\csc^2(\alpha z)}{2-i2\sigma^2\alpha\cot(\alpha z)}\right),\end{aligned} \tag{9a}$$

which corresponds to Fig. 1(a). From Eq. (9a), one can find that the beam envelope is periodic in z, and the period is π/α, which is in accordance with Eq. (4a).

4.2. Bessel–Gauss beams

As concerns the BG beams, we also begin with the case of an arbitrary order $\psi(x, 0) = \exp(-x^2/2\sigma^2)J_n(x)$. According to Eq. (7), we have

$$\psi(x, z) = (-i)^n \frac{f(x, z)}{\beta\sqrt{\pi}} \int_{-\pi/2}^{\pi/2} T_n(\sin\theta) \exp\left(-\frac{(K - \sin\theta)^2}{4\beta}\right) d\theta. \tag{9b}$$

Comparing Eq. (9b) with Eq. (3b), we find that they share the same oscillation period $\mathcal{D}_s$, hence Eq. (9b) will reduce to Eq. (3b) at an odd integer multiple of $\mathcal{D}_s/2$.

4.3. Finite-energy Airy beams

For the case shown in Fig. 1(c), one can also obtain the corresponding analytical solution with the input $\psi(x, 0) = \mathrm{Ai}(x)\exp(ax)$:

$$\begin{aligned}\psi(x, z) = & -f(x, z)\sqrt{i\frac{\pi}{b}} \exp\left(\frac{a^3}{3}\right) \mathrm{Ai}\left(\frac{K}{2b} - \frac{1}{16b^2} + i\frac{a}{2b}\right) \\ & \times \exp\left[\left(a + \frac{i}{4b}\right)\left(\frac{K}{2b} - \frac{1}{16b^2} + i\frac{a}{2b}\right)\right] \exp\left[-i\frac{K^2}{4b} - \frac{1}{3}\left(a + \frac{i}{4b}\right)^3\right].\end{aligned} \tag{9c}$$

Taking into account the asymmetry of the finite energy Airy beam, the period is $2\mathcal{D}_s \equiv \mathcal{D}_{\mathrm{as}}$. Note that Eq. (9c) is not valid when $z = (2m-1)\mathcal{D}_{\mathrm{as}}/4$, because at these positions $b = 0$. To obtain an analytical solution at $z = (2m - 1)\mathcal{D}_{\mathrm{as}}/4$ one must directly solve Eq. (7), which gives the result reported in Eq. (3c). Therefore, the solution for this case is a combination of Eqs. (3c) and (9c).

5. Self-Fourier beams

By now, it should be apparent that the propagation of beams according to the linear Schrödinger equation with parabolic potential is intimately connected with the self-Fourier (SF) transform. It is easy to find a beam, the FT of which is the beam itself—the Gaussian beam. Except Gaussians, other nontrivial functions have been found [35–40], such as HG functions and comb functions. In Eq. (8), $b = 0$ when $z = m\mathcal{D}_s/2$, with m being an odd integer, so that the equation is just a Fourier transform of HG beam without a parabolic chirp, and the solution is shown in Eq. (3a), which is also a HG beam. In fact, there are infinitely many SF beams, which are constructed according to the rule $f(x) = g(x) + g(-x) + \hat{g}(x) + \hat{g}(-x)$, where $g(x)$ is any Fourier-transformable function. This general rule was established a while ago by Caola [36] and the topic of SF beams by now is not new at all, as witnessed by the references cited above; still, we believe that the method on how to prepare novel SF beams introduced in this paper is not reported before and worthy of attention.

From Fig. 2, one can see that the intensity profiles in real and k spaces are the same in-between the points $z = m\mathcal{D}_s$ and $z = (2m + 1)\mathcal{D}_s/2$, where m is a non-negative integer. Considering that the system is linear and reciprocal, the places of interest should be $z = (2m + 1)\pi/(4\alpha)$. For simplicity, we choose $m = 0$. When the beam propagates to $z = \pi/4$, we have $b = \alpha/2$, $K = \sqrt{2}\alpha x$, and

$$f(x) = A\exp\left(i\frac{\alpha}{2}x^2\right), \quad \text{with } A = \sqrt{-i\frac{\alpha}{\sqrt{2}\pi}}.$$

Therefore, Eq. (7) can be rewritten as

$$\psi(x) = A\exp\left(i\frac{\alpha}{2}x^2\right) \int_{-\infty}^{+\infty} \psi(\xi) \exp\left(i\frac{\alpha}{2}\xi^2\right) \exp\left(-i\sqrt{2}\alpha x\xi\right) d\xi. \tag{10}$$

We let $g(x) = \exp(i\alpha x^2/2)$ and introduce the FT operator $\mathcal{F}[\circ](\bullet)$, in which $\circ$ and $\bullet$ represent the original function and the spatial frequency, respectively. Eq. (10) can be recast as

$$\psi(x) = Ag(x)\left\{\mathcal{F}[\psi(\xi)](K) \star \mathcal{F}[g(\xi)](K)\right\}, \tag{11}$$

where $\star$ represents the convolution operation, and the spatial frequency is K. Taking the FT of Eq. (16) with spatial frequency k, one finds

$$\begin{aligned}\mathcal{F}[\psi(x)](k) &= A\mathcal{F}[g(x)](k) \star \mathcal{F}[\mathcal{F}[\psi(\xi)](K) \star \mathcal{F}[g(\xi)](K)](k)\\ &= \frac{A}{8\alpha^2\pi^2}\mathcal{F}[g(x)](k) \star \left[\psi\left(-\frac{k}{\sqrt{2}\alpha}\right) g\left(-\frac{k}{\sqrt{2}\alpha}\right)\right]. \end{aligned} \tag{12}$$

After some algebra, Eq. (12) is rewritten in the form

$$\mathcal{F}[\psi(x)](k) = \frac{A}{8\alpha^2\pi^2}\sqrt{\frac{2i\pi}{\alpha}}\left[\exp\left(i\frac{\alpha}{2}\xi^2\right)\psi(\xi)\right] \star \exp\left(-i\alpha\xi^2\right), \tag{13}$$

in which we let $k = -\sqrt{2}\xi\alpha$. The convolution in Eq. (13) can be written as

$$\frac{1}{2\pi}\exp\left(-i\alpha x^2\right)\int_{-\infty}^{+\infty}\psi(\xi)\exp\left(-i\frac{\alpha}{2}\xi^2\right)\exp\left(i2\alpha x\xi\right)d\xi.$$

If one assumes $x = ix'/\sqrt{2}$ and $\xi = i\xi'$, the convolution is finally put in the form

$$\frac{i}{2\pi}\exp\left(i\frac{\alpha}{2}x'^2\right)\int_{-\infty}^{+\infty}\psi(\xi')\exp\left(i\frac{\alpha}{2}\xi'^2\right)\exp\left(-i\sqrt{2}\alpha x'\xi'\right)d\xi', \tag{14}$$

which is just the integral in Eq. (10). Therefore, the beam envelopes in real and inverse spaces have the same profile (up to a transverse scaling), i.e. the beams represented by Eq. (10) are the SF beams. In light of the fact that the initial beam can be arbitrary, the number of SF beams is infinite and can be easily made. *Generally, for an arbitrary $\psi(x)$ propagating to $\pi/(4\alpha)$ in a parabolic potential, a self-Fourier beam will be obtained.* Note that if the initial beam is parity-asymmetric, the corresponding FT still has the same profile, but with an intermediate inversion. In general, the corresponding FT pair is

$$\mathcal{F}[\psi(x)](k) = \sqrt{\frac{2\pi}{\alpha}}\psi\left(-\frac{k}{\alpha}\right). \tag{15}$$

We would like to emphasize that this method is completely different from the previously reported methods. Its discovery is enabled by the useful properties of beam propagation in a parabolic potential.

As an example, we discuss the finite energy Airy beam $\psi(x, z=0) = \mathrm{Ai}(x)\exp(ax)$ with $a = 0.1$ as an initial beam in a parabolic potential. Plugging this beam in Eq. (7), one obtains the corresponding SF beam at $z = \pi/(4\alpha)$, written as

$$\begin{aligned}\psi(x) = &-\sqrt[4]{2}\,\mathrm{Ai}\left(\sqrt{2}x - \frac{1}{4\alpha^2} + i\frac{a}{\alpha}\right)\exp\left[a\left(\sqrt{2}x - \frac{1}{2\alpha^2}\right)\right]\\ &\times\exp\left[-\frac{i}{2}\left(2\alpha x^2 - \frac{\sqrt{2}}{\alpha}x + \frac{a^2}{\alpha} + \frac{1}{6\alpha^3}\right)\right]. \end{aligned} \tag{16}$$

In Fig. 4, the intensity of the SF beam is shown by the black curve, and the corresponding intensity in Fourier space is shown by the red curve. One can see that the beam profiles are the same except for an inversion, which is in accordance with the theoretical result presented in Eq. (15).

Naturally, the harmonic oscillator model in Eq. (1) is easily extended to two, three or even four dimensions. The hydrogen atom in three dimensions can be represented as a four-dimensional harmonic oscillator [41]. Specifically, in two dimensions the problem can be reduced by the separation of variables to two one-dimensional cases [15]. In Fig. 5(a1) (real space) and Fig. 5(b1) (inverse space), we display the results for a two-dimensional finite-energy Airy beam [4]

$$\psi(x, y, z=0) = \mathrm{Ai}(x)\mathrm{Ai}(y)\exp[a(x+y)].$$

As expected, the beam at $z = \pi/4$ is a SF beam, and the corresponding analytical solution can be obtained immediately from Eq. (16)—by making a product of x and y components.

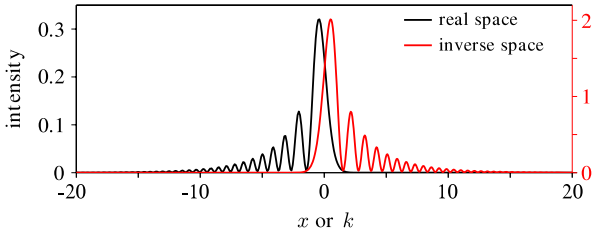

Fig. 4. (Color online) Comparison of intensities of an AB at $z = \pi/4$ in real space and inverse space, corresponding to Fig. 2(a). Intensities in real and frequency spaces refer to the left and right y scales, respectively.

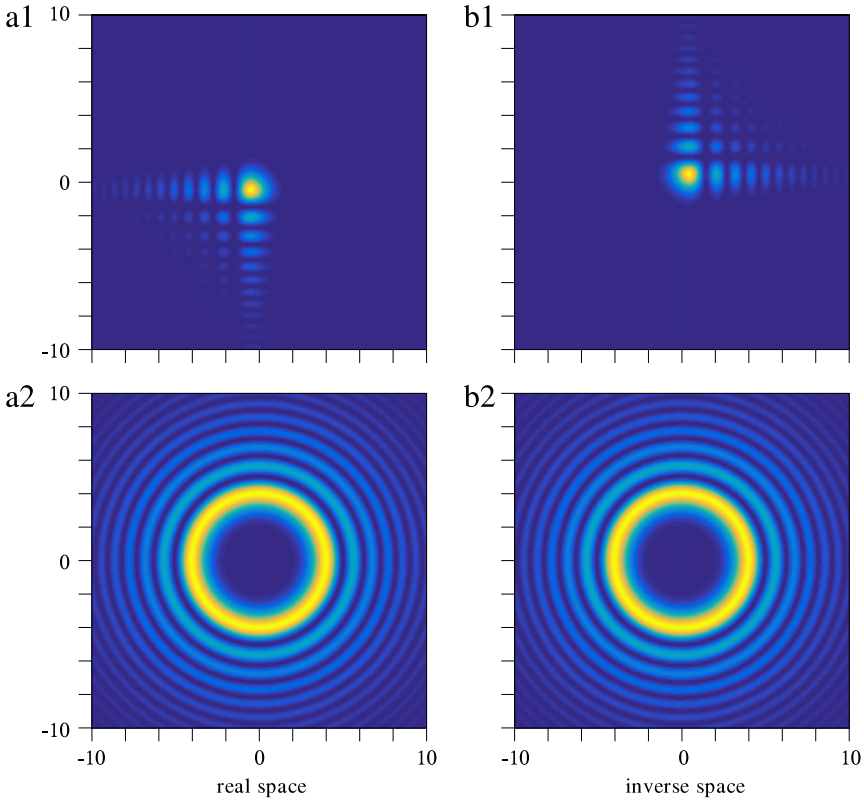

Fig. 5. (Color online) (a1) Intensity of a two-dimensional finite-energy Airy beam $\mathrm{Ai}(x)\mathrm{Ai}(y)\exp[a(x+y)]$ at $z = \pi/4$ in the real space. (b1) The corresponding intensity in the inverse space. (a2) and (b2) Same as (a1) and (b1), but for a circular finite-energy Airy beam $\psi(x, y, z = 0) = \mathrm{Ai}(r_0 - r)\exp[a(r_0 - r)]$. The parameters are $\alpha = 1$, $r_0 = 5$, and $a = 0.1$.

In addition to the inputs with separated variables, one can also treat two-dimensional inputs with non-separable variables, for example, an outward circular finite-energy Airy beam [42,43]. Such an initial beam can be written in polar coordinates as

$$\psi(x, y, z = 0) = \mathrm{Ai}(r_0 - r)\exp[a(r_0 - r)],$$

where r_0 determines the location of the main ring. As shown in Fig. 5(a2) and (b2), the beam at $z = \pi/4$ is still a SF beam. However, the corresponding explicit analytical solution cannot be obtained, which is true for most of the initial beams. Still, the method is valid for all kinds of initial beams, regardless of whether the results can be expressed explicitly or not.

6. Conclusion and outlook

In conclusion, we have theoretically and numerically investigated the beam propagation in a linear medium with an external parabolic potential. According to this model, the beam will undergo profile oscillation during propagation, which will suppress diffraction. For an asymmetric beam, such as the finite energy AB, there is a periodic inversion during propagation. The oscillation period for parity-symmetric beams is half that of parity-asymmetric beams.

We also find that an arbitrary beam realizes automatic FT during propagation. At half the period for parity-symmetric beams and a quarter of the period for parity-asymmetric beams, the FT of the initial beams is obtained repeatedly; at the places in between, the beam is the FT of the initial beam with a parabolic chirp.

Last but not least, based on the theoretical model, we discover a class of SF beams. This method may be easily implemented in experiment—one can use a GRIN medium or a Lohmann optical system [44,34], which are extensively investigated and well understood. The properties discussed not only exhibit the importance of parabolic potential in linear optics, but broaden the understanding of recurrence in the paraxial beam propagation, and also exemplify scientific significance of the parabolic potential propagation for signal processing, imaging, microparticle manipulation, information storage, and other applications.

In the end, we mention some of the useful extensions of the theory presented here. In addition to GRIN media, to which the theory applies directly, Bose–Einstein condensates with harmonic traps [45,46] are viable candidates, when the nonlinearity is weak [47,48]. Talbot effect in one and two dimensions can also be presented as a SF phenomenon—in fact, as a fractional FT [39,18]. A big challenge would be to extend these ideas to nonlinear domain—which in principle is difficult, since FT by itself is a linear operation. Nonetheless, we have recently demonstrated [49,50] that the nonlinear Talbot effect can be presented in terms of primary and secondary recurrences, which might be interpreted as SF phenomena. Quite surprisingly, it is also proven that the hyperbolic secant function – one of the workhorses in soliton theory – is a SF function [40].

Acknowledgments

This work was supported by the 973 Program (2012CB921804), KSTIT of Shaanxi province (2014KCT-10), NSFC (61308015, 11474228), NSFC of Shaanxi province (2014JQ8341), CPSF (2014T70923, 2012M521773), and the NPRP 6-021-1-005 project of the Qatar National Research Fund (a member of the Qatar Foundation).

References

[1] F. Lederer, G.I. Stegeman, D.N. Christodoulides, G. Assanto, M. Segev, Y. Silberberg, Phys. Rep. 463 (1–3) (2008) 1–126.
[2] I.L. Garanovich, S. Longhi, A.A. Sukhorukov, Y.S. Kivshar, Phys. Rep. 518 (1–2) (2012) 1–79.
[3] U. Peschel, T. Pertsch, F. Lederer, Opt. Lett. 23 (21) (1998) 1701–1703.
[4] G.A. Siviloglou, D.N. Christodoulides, Opt. Lett. 32 (8) (2007) 979–981.
[5] I. Kaminer, R. Bekenstein, J. Nemirovsky, M. Segev, Phys. Rev. Lett. 108 (16) (2012) 163901.
[6] G.A. Siviloglou, J. Broky, A. Dogariu, D.N. Christodoulides, Phys. Rev. Lett. 99 (21) (2007) 213901.
[7] C. Hang, Z. Bai, G. Huang, Phys. Rev. A 90 (2) (2014) 023822.
[8] Y.Q. Zhang, M.R. Belić, J. Sun, H.B. Zheng, Z.K. Wu, H.X. Chen, Y.P. Zhang, Rom. Rep. Phys. 67 (3) (2015) 1099–1107.
[9] F. Diebel, B.M. Bokić, D.V. Timotijević, D.M.J. Savić, C. Denz, Opt. Express 23 (19) (2015) 24351–24361.
[10] W.-P. Zhong, M. Belić, Y.Q. Zhang, Opt. Express 23 (18) (2015) 23867–23876.
[11] W. Liu, D.N. Neshev, I.V. Shadrivov, A.E. Miroshnichenko, Y.S. Kivshar, Opt. Lett. 36 (7) (2011) 1164–1166.
[12] Z. Ye, S. Liu, C. Lou, P. Zhang, Y. Hu, D. Song, J. Zhao, Z. Chen, Opt. Lett. 36 (16) (2011) 3230–3232.
[13] N.K. Efremidis, Opt. Lett. 36 (15) (2011) 3006–3008.
[14] M.A. Bandres, J.C. Gutiérrez-Vega, Opt. Express 15 (25) (2007) 16719–16728.
[15] Y.Q. Zhang, M.R. Belić, L. Zhang, W.P. Zhong, D.Y. Zhu, R.M. Wang, Y.P. Zhang, Opt. Express 23 (8) (2015) 10467–10480.
[16] Y.Q. Zhang, X. Liu, M.R. Belić, W.P. Zhong, F. Wen, Y.P. Zhang, Opt. Lett. 40 (16) (2015) 3786–3789.
[17] G. Zhou, R. Chen, X. Chu, Appl. Phys. B 109 (4) (2012) 549–556.
[18] D. Mendlovic, H.M. Ozaktas, J. Opt. Soc. Am. A 10 (9) (1993) 1875–1881.
[19] D. Mendlovic, H.M. Ozaktas, A.W. Lohmann, Appl. Opt. 33 (26) (1994) 6188–6193.
[20] C. Gomez-Reino, M.V. Perez, C. Bao, Gradient-index Optics: Fundamentals and Applications, Springer, Berlin, 2002.
[21] A.W. Snyder, D.J. Mitchell, Science 276 (5318) (1997) 1538–1541.
[22] D. Lu, W. Hu, Y. Zheng, Y. Liang, L. Cao, S. Lan, Q. Guo, Phys. Rev. A 78 (4) (2008) 043815.

[23] G. Zhou, R. Chen, G. Ru, Laser Phys. Lett. 11 (10) (2014) 105001.
[24] M. Shen, J. Gao, L. Ge, Sci. Rep. 5 (2015) 9814.
[25] Y.Q. Zhang, M. Belić, Z.K. Wu, H.B. Zheng, K.Q. Lu, Y.Y. Li, Y.P. Zhang, Opt. Lett. 38 (22) (2013) 4585–4588.
[26] Y.Q. Zhang, M.R. Belić, H.B. Zheng, H.X. Chen, C.B. Li, Y.Y. Li, Y.P. Zhang, Opt. Express 22 (6) (2014) 7160–7171.
[27] R. Driben, Y. Hu, Z. Chen, B.A. Malomed, R. Morandotti, Opt. Lett. 38 (14) (2013) 2499–2501.
[28] J. Rogel-Salazar, H.A. Jiménez-Romero, S. Chávez-Cerda, Phys. Rev. A 89 (2) (2014) 023807.
[29] S. Ponomarenko, G. Agrawal, Phys. Rev. Lett. 97 (1) (2006) 013901.
[30] W. Zhong, L. Yi, Phys. Rev. A 75 (6) (2007) 061801.
[31] B. Yang, W.-P. Zhong, M.R. Belić, Commun. Theor. Phys. 53 (5) (2010) 937–942.
[32] C. Bernardini, F. Gori, M. Santarsiero, Eur. J. Phys. 16 (2) (1995) 58–62.
[33] A.A. Kovalev, V.V. Kotlyar, S.G. Zaskanov, J. Opt. Soc. Am. A 31 (5) (2014) 914–919.
[34] H.M. Ozaktas, Z. Zalevsky, M.A. Kutay, The Fractional Fourier Transform with Applications in Optics and Signal Processing, Wiley, New York, 2001.
[35] G. Cincotti, F. Gori, M. Santarsiero, J. Phys. A: Math. Gen. 25 (20) (1992) L1191–L1194.
[36] M.J. Caola, J. Phys. A: Math. Gen. 24 (19) (1991) L1143–L1144.
[37] S.G. Lipson, J. Opt. Soc. Am. A 10 (9) (1993) 2088–2089.
[38] T.P. Horikis, M.S. McCallum, J. Opt. Soc. Am. A 23 (4) (2006) 829–834.
[39] A.W. Lohmann, D. Mendlovic, J. Opt. Soc. Am. A 9 (11) (1992) 2009–2012.
[40] P.P. Banerjee, T.-C. Poon, J. Opt. Soc. Am. A 12 (2) (1995) 425–426.
[41] F.H.J. Cornish, J. Phys. A: Math. Gen. 17 (2) (1984) 323–327.
[42] P. Zhang, J. Prakash, Z. Zhang, M.S. Mills, N.K. Efremidis, D.N. Christodoulides, Z. Chen, Opt. Lett. 36 (15) (2011) 2883–2885.
[43] I. Chremmos, P. Zhang, J. Prakash, N.K. Efremidis, D.N. Christodoulides, Z. Chen, Opt. Lett. 36 (18) (2011) 3675–3677.
[44] J.W. Goodman, Introduction to Fourier Optics, third ed., Roberts and Company Publishers, Inc., 2005.
[45] D. Mihalache, Rom. J. Phys. 59 (2014) 295–312.
[46] V.S. Bagnato, D.J. Frantzeskakis, P.G. Kevrekidis, B.A. Malomed, D. Mihalache, Rom. Rep. Phys. 67 (1) (2015) 5–50.
[47] S. Skupin, U. Peschel, L. Bergé, F. Lederer, Phys. Rev. E 70 (1) (2004) 016614.
[48] Y.Q. Zhang, S. Skupin, F. Maucher, A.G. Pour, K.Q. Lu, W. Królikowski, Opt. Express 18 (26) (2010) 27846–27857.
[49] Y.Q. Zhang, M. Belić, H.B. Zheng, H.X. Chen, C.B. Li, J.P. Song, Y.P. Zhang, Phys. Rev. E 89 (3) (2014) 032902.
[50] Y.Q. Zhang, M.R. Belić, M.S. Petrović, H.B. Zheng, H.X. Chen, C.B. Li, K.Q. Lu, Y.P. Zhang, Phys. Rev. E 91 (3) (2015) 032916.